Alginate-derived hydrogels synergetic with metal-phenolic nanospheres for chronic wound therapy

Donghai Li [a], Mengzhu Li [b], Liangyu Wang [a], Jie Zhang [c], Xiaoyue Wang [c]*, Jun Nie [a], and Guiping Ma [a]*

a Beijing Laboratory of Biomedical Materials, Beijing University of Chemical Technology, Beijing 100029, P. R. China.

b China Academy of Aerospace Science and Innovation, Beijing 100176,China

c Department of Gastroenterology, Beijing Anzhen Hospital, Capital Medical University, Beijing 100029, China

Corresponding Author

Guiping Ma* E-mail: magp@mail.buct.edu.cn

Keywords: alginate, supramolecular interaction, metal-phenolic, macrophage polarization, diabetic wound

Experimental part

1. Preparation of TFCN

A certain amount of tannic acid (7mg) was ultrasonically dissolved in deionized water (7mL), and then sodium hydroxide (10μL, 0.05M) was added to the tannic acid solution under low speed stirring to obtain an alkaline solution of tannic acid. Then the phenolic metal coordination was performed by adding 15μL $FeCl_3 \cdot 6H_2O$ aqueous solution (2.5wt%) under stirring condition. After 30 minutes, the reaction mixture was centrifuged at 8000 RPM for 5 minutes, washed in deionized water for 3 times, and finally freeze-dried to obtain tannic-iron metal-phenol complex (TFCN). The molar ratio of TA/Fe^{3+} was 3:1.

2. Characterizations

The 1HNMR spectra of sodium alginate grafted with aminophenylboric acid were determined by 400MHz nuclear magnetic resonance spectrometer (AVANCEIII) with deuterated water as solvent. The FTIR spectra of Alg, ALG-PBA, TFCN-Alg-PBA/PVA samples were analyzed by Fourier Transform infrared spectrometer (NICOLET-5700) in the range of 400~4000cm^{-1}.Uv-vis spectra of Alg, ALG-PBA and TFCN at different pH were recorded by UV spectrophotometer (UV, 2310II, China) in the range of

200~800nm.The particle size and Zeta potential of TFCN with different molar ratios were characterized by light scattering particle size and Zeta potentiometer (ZS90).

X-ray diffraction (XRD, Ultima IV) was employed to identify the amorphous nature of TFCN .X-ray photoelectron spectroscopy(XPS ESCALAB 250) was performed to analyze the elemental composition and chemical valence states of TFCN. Field emission scanning electron microscopy (SEM, S-4700, Hitachi, Japan) was used to observe the surface and cross-section of the hydrogel. The mechanical properties of the gel under rheology were investigated by TA rotating rheometer (DHR-1).Specifically, a parallel plate clamp with a diameter of 20mm is selected, and the test distance is 50mm. Subsequently, a dynamic time sweep mode was employed, with small strain (γ = 1%) and large strain (γ = 1050%), at a temperature of 25°C and an oscillation frequency of 10 rad/s. Four consecutive cycles of alternating strain sweeps were performed, with each strain sweep lasting 200 seconds. Changes in the storage modulus and loss modulus were recorded. In addition, the hydrogel was cut in half by the external force of physical cutting to heal itself at a set time, and the healing of the section was observed through a microscope at the micro level. The hydrogel was put into a glass bottle containing bracelet beads of different sizes, and the situation of the gel filling irregular space at different times was filmed to investigate the shape adaptability of the gel. The viscosity of the gel was recorded by TA rotating rheometer (DHR-1) in dynamic frequency scanning mode to verify the injectivity of the gel.

3. Free radical scavenging experiments of $TFCN_x$-Alg-PBA/PVA hydrogels

The antioxidant activity of the gel was evaluated by 1, 1-diphenyl-2-trinitrophenylhydrazine (DPPH) radical scavenging method. The measured hydrogel material was added to the ethanol solution of DPPH (10mL125uM) in a dark environment. The preset incubation time in dark environment was used to measure the absorbance (A_e) of the solution at 517nm by UV-vis ultraviolet spectrophotometer. The absorbance (A_b) of pure DPPH solution was used as a blank control. The following formula is used to calculate the scavenging efficiency of DPPH free radicals[1]

$$\text{DDPH scavenging}(\%) = \frac{A_b - A_e}{A_b} \times 100\%$$

In addition, the antioxidant capacity of the hydrogel was further evaluated by ABTS

free radical scavenging. The specific steps are as follows: A 200 μL volume of ABTS solution was mixed with an equimolar amount of oxidizing agent solution. The resulting mixture was kept in a light-protected environment at room temperature for 16 hours, leading to the formation of the ABTS working solution. Then dilute it with 80% ethanol until the absorbance of the working liquid A746 is 0.7±0.05.The hydrogel material was added to the diluted working solution under light-shielded conditions and subjected to a predetermined incubation period. Subsequently, the absorbance (A_e) of the solution at 746 nm was quantified using a UV-vis ultraviolet spectrophotometer. The absorbance (A_b) of pure ABTS working fluid was used as a blank control. The scavenging efficiency of ABTS free radicals was calculated using the following formula[1].

$$\text{ABTS* scavenging}(\%) = \frac{A_b - A_e}{A_b} \times 100\%$$

4. Biocompatibility test

4.1 In vitro cell assay

The in vitro cytotoxicity of hydrogels was determined by CKK-8 method. Mouse fibroblasts L929 were inoculated into 96-well plates containing 100μL medium, cell density was maintained at 5×10^3 cells per well, and cultured in a 5%CO_2 (v/v) sterile environment at 37℃ for 12h. The gel samples of the experimental group were taken as suspensions consisting of different concentrations (0.02, 0.05, 0.1, 0.4, 0.8, 1mg/mL) and added dropwise for 10μL into 96-well plates containing L929 cells. while the blank control group was added 10μL PBS buffer and incubated for 24 hours in a sterile environment at 37℃.Finally, 10μL CCK-8 solution was added to each well and cultured for 2 hours. The absorbance at 450nm was measured, and the cell survival rate was calculated according to the cell viability (CV) formula[2].

$$\text{CV}(\%) = \frac{A_e}{A_c} \times 100\%$$

Where A_e is the absorbance of the experimental group and A_c is the absorbance of the blank control group

4.2 Live/dead fluorescent staining experiment

5μL 16mM PI (propyl iodide) solution was added to 10mL PBS solution, and the vortex was uniform to obtain 8uM PI stock solution. Add 5μL 4mM of AM (calcein) stock solution into 10mL of PI solution and vortex mixing to get the working solution. Cells were stained with working solution (2uM calcein, 8uM pyridine iodide).The living and dead cells at different times (1,3,5 days) were observed by confocal fluorescence inverted microscope.

4.3 Cell migration and adhesion experiment

Mouse fibroblasts L929 were inoculated into 6-well plates with a cell density of 5×10^5 cells per well, and incubated at 37℃ for 24h to form cell layers. The pipette tip was then cut perpendicular to the surface of the cell layer to create scratches, and the gel material was added to the scratches after washing twice with sterile PBS. The cell migration was recorded by inverted fluorescence microscope at 12,24 h. Image J was used for analysis and processing, and the following formula was used to calculate cell mobility[3].

$$\text{Migration rate}(\%)=\frac{w_i - w_t}{w_i}$$

Where w_i represents the initial scratch area at 0 hours and w_t represents the scratch area at T hours of culture (t=12h or 24h)

The sterilized hydrogel sample was mixed with cell suspension of L929 (5×10^4/mL), and the control group was tissue culture polystyrene (TCPS).After incubation for 24 hours, remove the medium and wash gently with PBS. The hydrogel was placed in a new 24-well plate and incubated with fluorescein diacetate solution (5mg/mL) for 5 minutes. Finally, the cells were washed twice with PBS and observed by inverted fluorescence microscope.

4.4 In vitro hemolysis test

Fresh blood was taken from the hearts of SD rats and placed in EDTA anticoagulant collection vessels. After standing for a period of time, 2mL of blood was taken and added to 3mL of 0.01m PBS buffer solution, centrifuged at 3000rpm for 5 minutes. The supernatant was discarded and the solution was supplemented to 5mL, and washing was repeated three times until there was no obvious red color in the serum. The centrifuged blood cells were then diluted to 2% with 0.01M of PBS buffer. A certain mass of hydrogel was mixed with 2% red blood cell suspension, and the final concentration was configured

as 2mg/mL, 4mg/mL, 8mg/mL, 16mg/mL. The negative control group was 2% erythrocyte suspension diluted with PBS buffer and the positive control group was 3% erythrocyte suspension containing TritionX-100. All the samples were incubated at 37℃ for 30min, and then centrifuged at 3000rpm for 5 min. The supernatant was taken and the absorbance at 540m was measured by UV-vis ultraviolet spectrophotometer. The hemolysis rate was calculated according to the formula of hemolysis rate[4]

$$\text{hemolysis (\%)} = \frac{A_e - A_n}{A_P - A_n} \times 100\%$$

In the formula, A_e, A_p and A_n are respectively the absorbance of the sample, positive and negative control group at 540nm.

4.5 Measurement of photothermal properties of TFCN &TFCN$_x$-Alg-PBA/PVA hydrogel

To evaluate the photothermal properties of TFCN, we used 808nm near-infrared laser (1W/cm^2) radiation to fill a centrifuge tube with 1mL of complex solution. The photothermal performance of complexes with varying concentrations (0.2, 0.4, 0.6, 0.8, 1 mg/mL) at the same power, as well as complexes with the same concentration (1 mg/mL) but different powers (0.6W, 0.8W, 1W, 1.2W, 1.5W), was investigated. The thermal map was taken with the infrared thermal imaging camera at the set time. In addition, under the same power density conditions (1W/cm^2), the TFCN complex (concentration 0.6mg/mL) was heated and cooled for 5 times. According to the reported method[5], a cycle curve was selected to calculate the photothermal conversion efficiency of the TFCN complex. The calculation formula is as follows:

$$\eta = \frac{hs \cdot (T_{max} - T_{surr}) - Q_{dis}}{I^{(1 - 10^{-A_{808}})}}$$

h is the heat transfer coefficient, s is the surface area of the container, Q_{dis} represents laser heat dissipation mediated by solvents and containers. I is the laser power and A is the absorbance at 808nm. T_{max} is the highest temperature of the sample during the cycle, and T_{surr} is the ambient temperature. Where hs can be obtained according to the following

formul

$$\theta = \frac{(T - T_{surr})}{T_{max} - T_{surr}}, \quad t = -\tau_S \ln \theta, \quad hs = \frac{mC_{water}}{\tau_S}$$

T is the temperature of the sample at different times, and $C_{water}$is the specific heat capacity of water

In order to evaluate the photothermal effect of the gel materials, gel samples with different concentrations (Percentage of TFCN:1.1%, 1.5%, 2.2%, 3%, 4.5%) of TFCN were irradiated with a near-infrared laser emitter (808nm, GCI-0901) (radiation conditions were 1W/cm^2, 300s).Thermal maps of the hydrogel are captured using an infrared thermal imaging camera. In order to further evaluate the photothermal effect of the gel, we selected a gel sample with a TFCN Percentage of 2.2% for four heating and cooling cycles, and conducted radiation tests at different power densities.

5. Histological and immunohistochemical analysis

Wound tissues of different groups of T1DM C57BL/6J mice were collected at 3, 5 and 11 days after surgery. 4% paraformaldehyde was fixed overnight, paraffin was embedded and sliced, and histopathological analysis was performed on the embedded sections. Hematoxylin-eosin (H&E) and Masson staining were used to quantitatively evaluate the closure of wound tissue and collagen deposition. Interleukin IL-6, IL-10 and platelet endothelial cell adhesion molecule CD31 were recorded by immunohistochemistry to study wound inflammation, epidermal regeneration and angiogenesis. In order to study the infiltration of macrophages, phenotypic polarization and proliferation of wound cells in T1DM mice, immunofluorescence imaging and analysis of CD86 and CD206 macrophage marker factors were also performed. All animal experiments are conducted in strict accordance with the National Institutes of Health "Guidelines for the Care and Use of Laboratory Animals" (NIH Publication No.8023, revised 1978) and approved by the Animal Ethics Committee of Beijing Anzhen Hospital, Capital Medical University (Ethics number:2022163X).

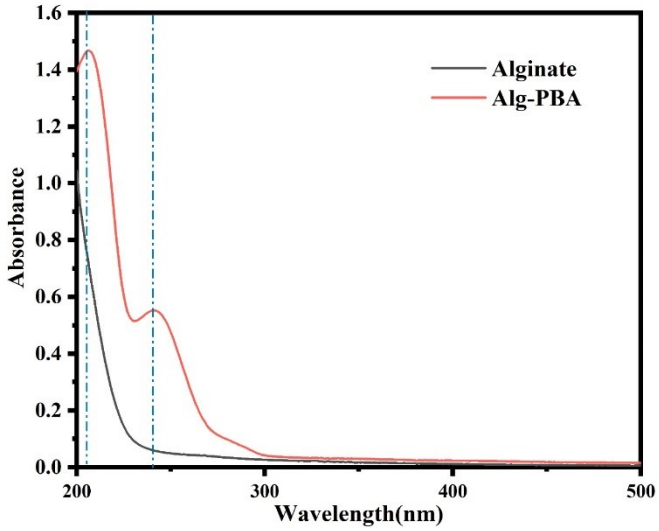

Figure S1 UV absorption spectra of Alg and Alg-PBA

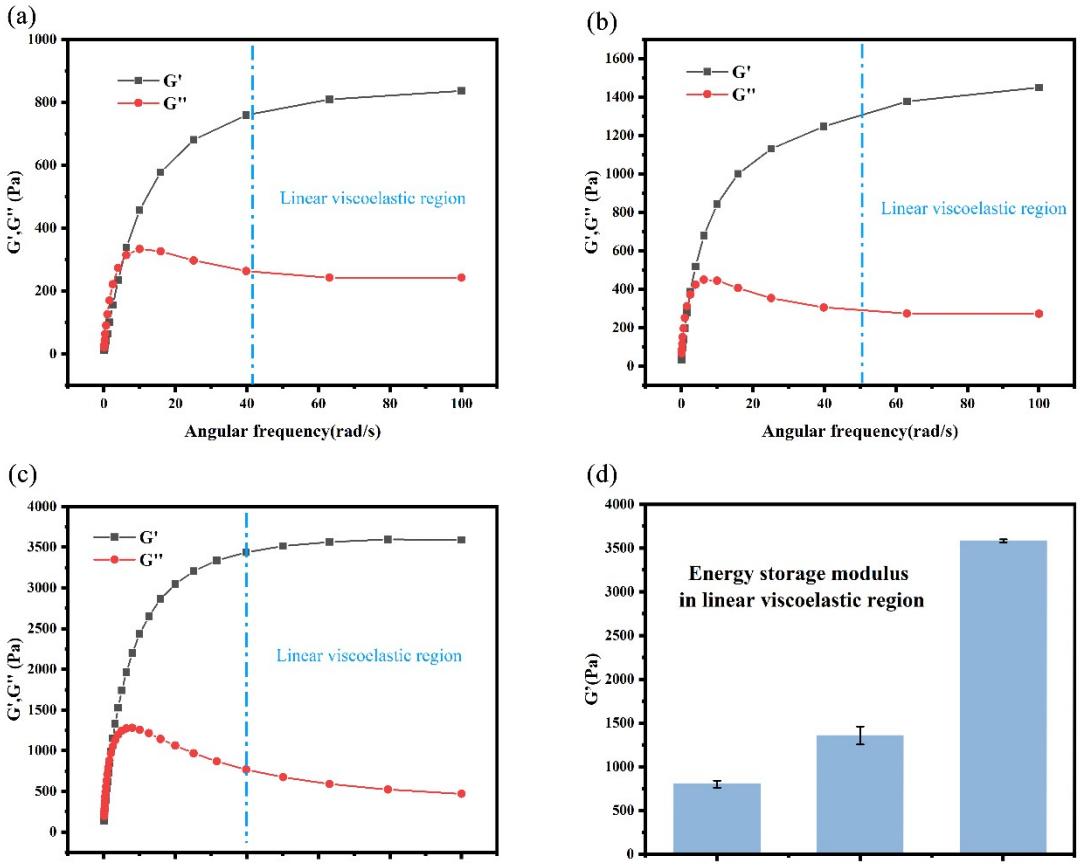

Figure S2 Rheological data of hydrogel of different proportions

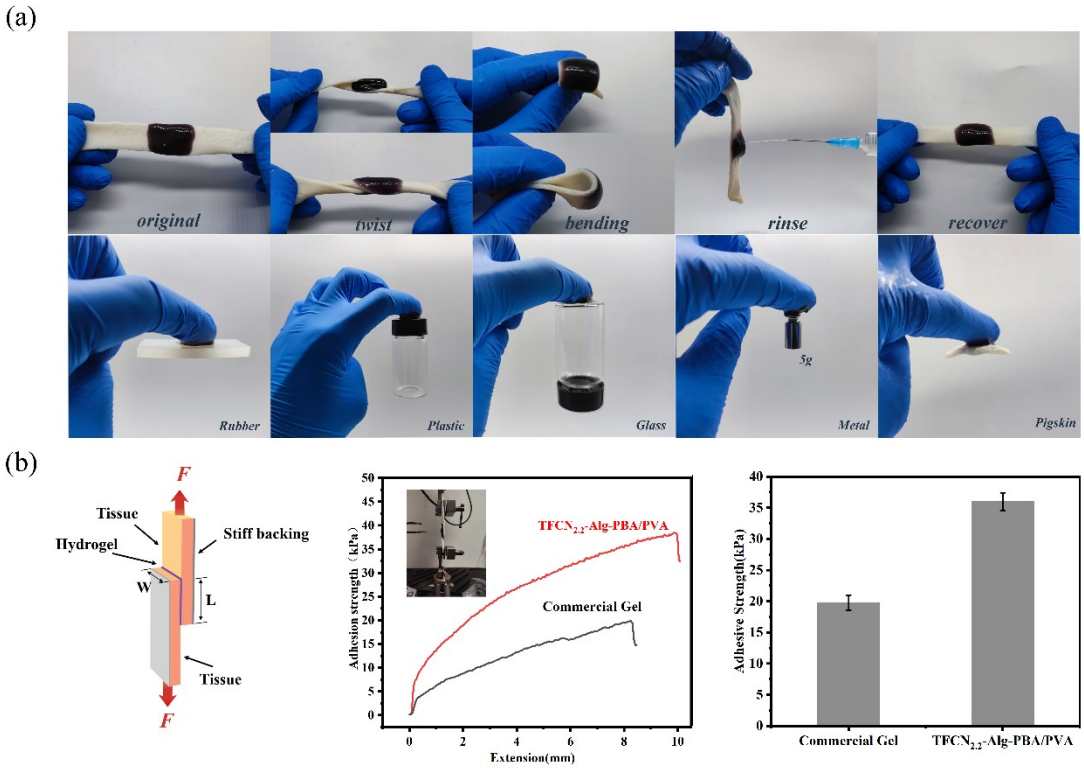

Figure S3 Photographs of hydrogels adhered to different substrates and their shear adhesion data

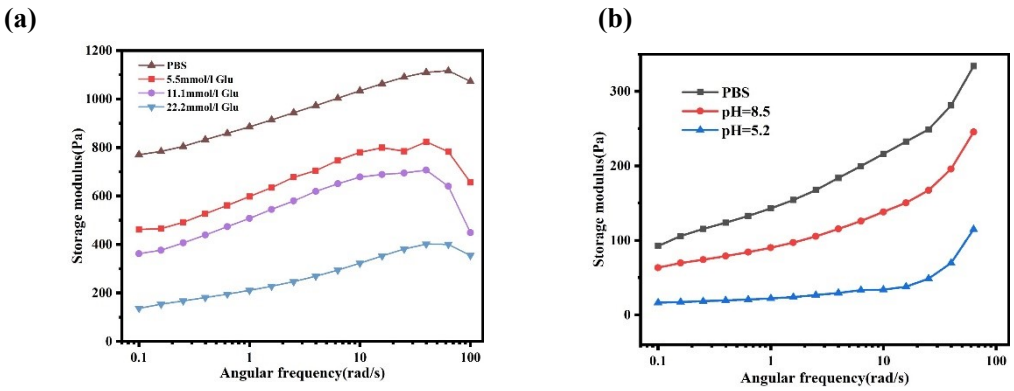

Figure S4 Rheological testing of hydrogels under different glucose concentrations and pH conditions

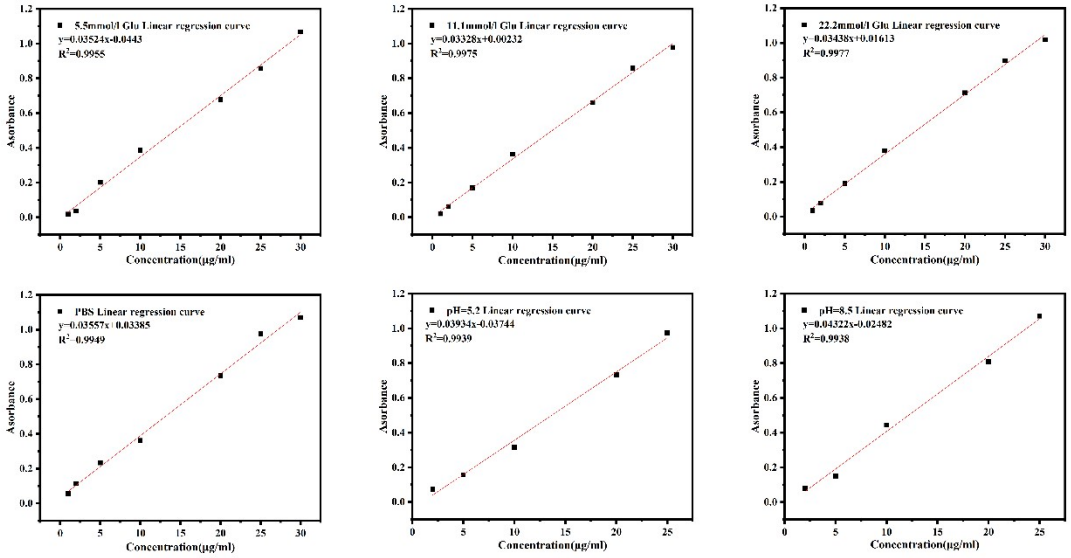

Figure S5 UV calibration curves of TA under different conditions

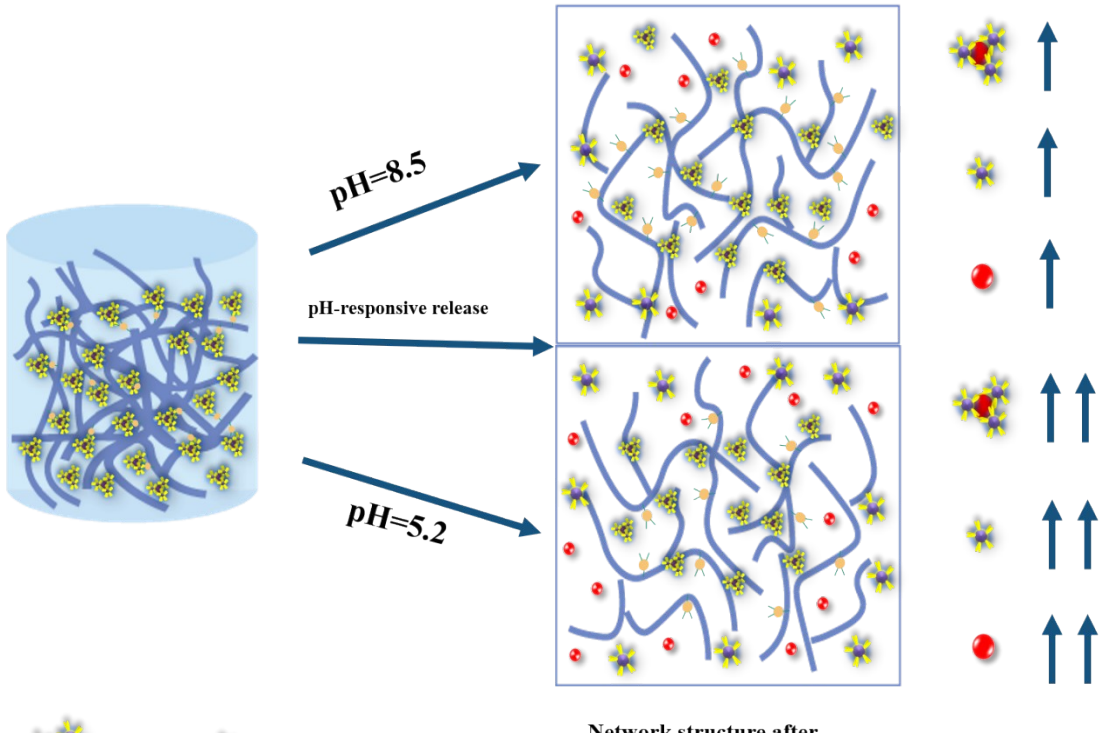

Figure S6 Illustration of pH-responsive TFCN release mechanism from TFCN-Alg-PBA/PVA

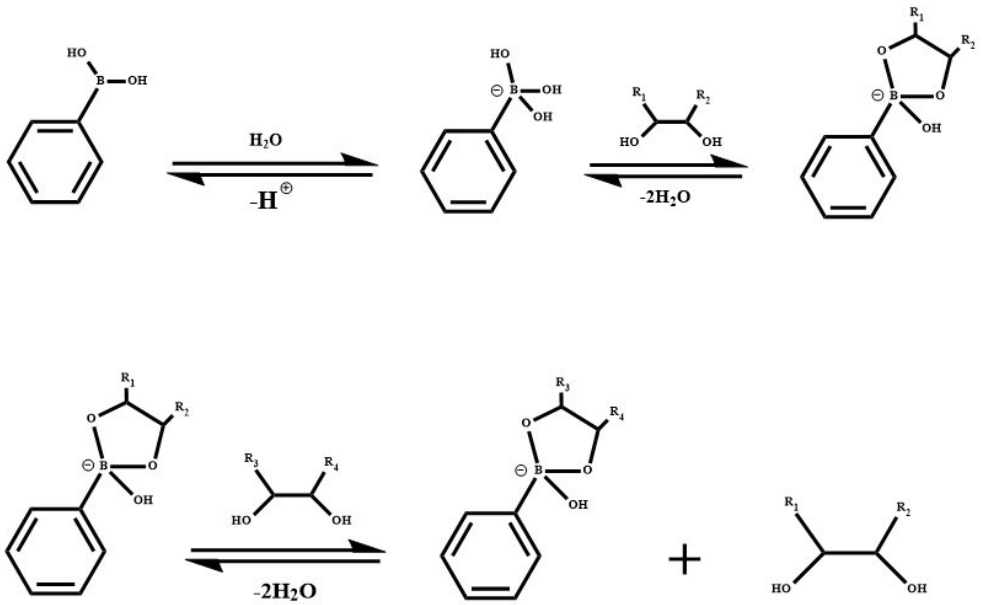

Figure S7 Illustration the Selective coordination mechanism of reversible borate ester bonds

(a)

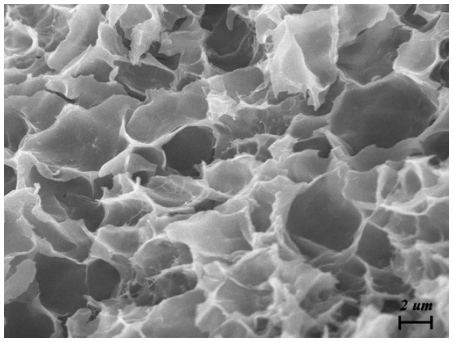

(b)

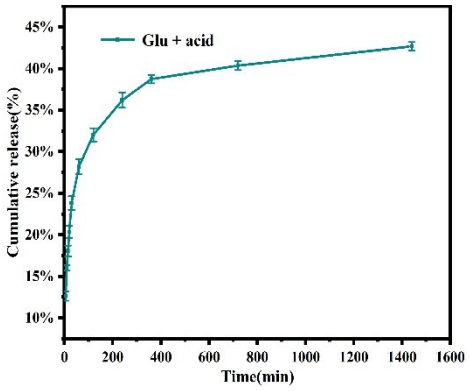

Figure S8 SEM morphology and TA release statistics of hydrogels under dual glucose and pH stimulation (n=3)

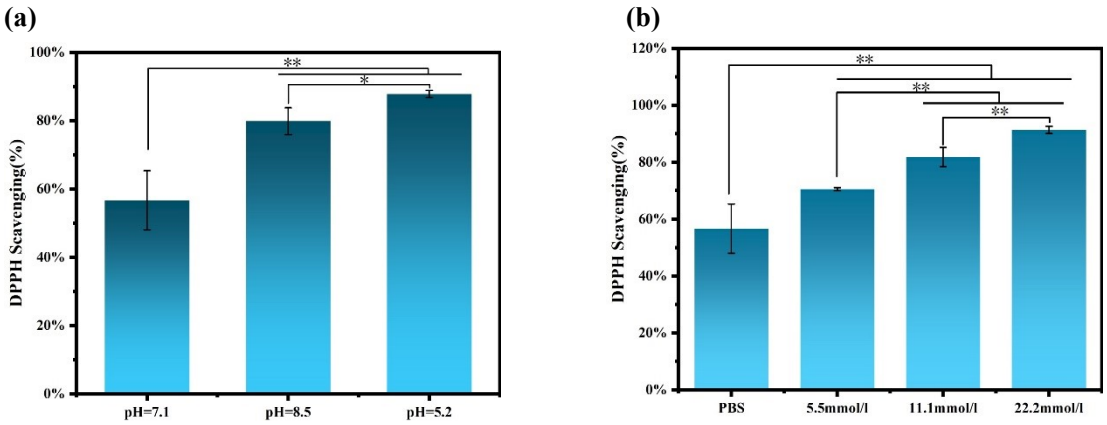

Figure S9 Scavenging rate of DPPH radicals by releasing TA equivalents under different stimuli (n=3)

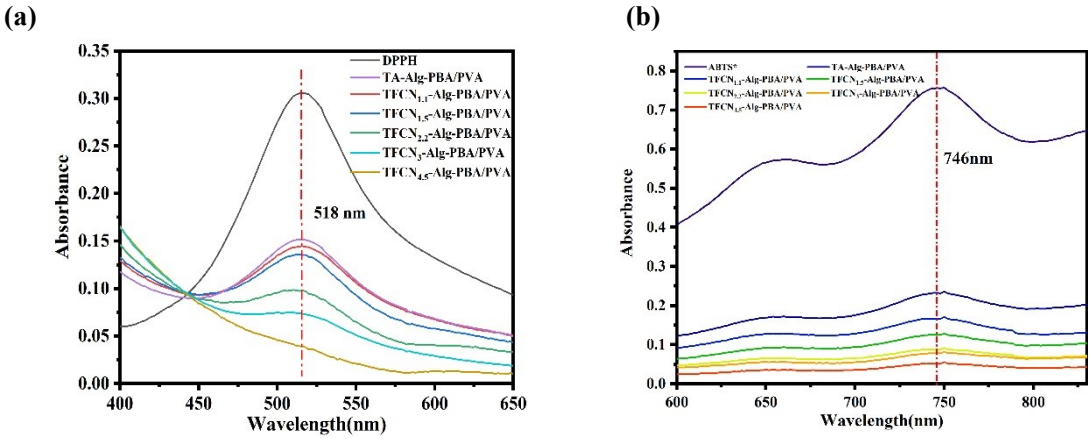

Figure S10 UV spectra of the effect of different hydrogels on the scavenging of DPPH and ABTS radicals

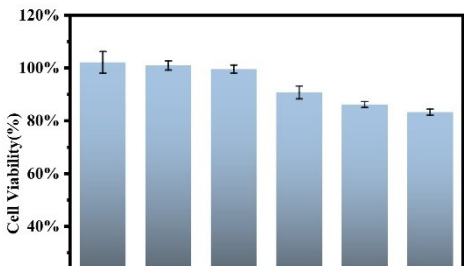

Figure S11 Cytotoxicity statistics of different concentrations of $TFCN_{2.2}$-Alg-PBA/PVA hydrogels

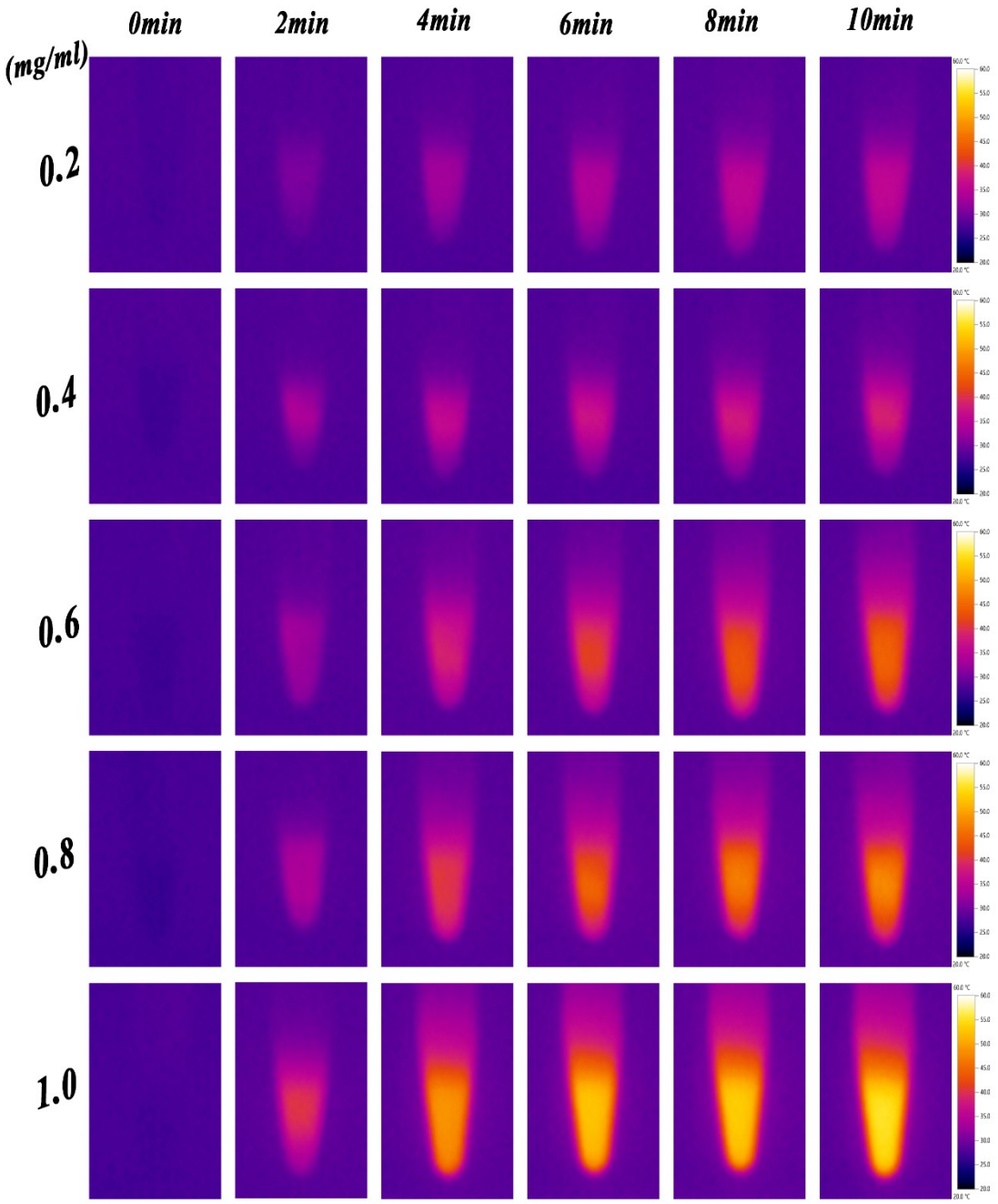

Figure S12 Infrared thermograms of TFCN solutions with different concentrations under 808 near-infrared laser radiation(5min/1.0 W cm^2)

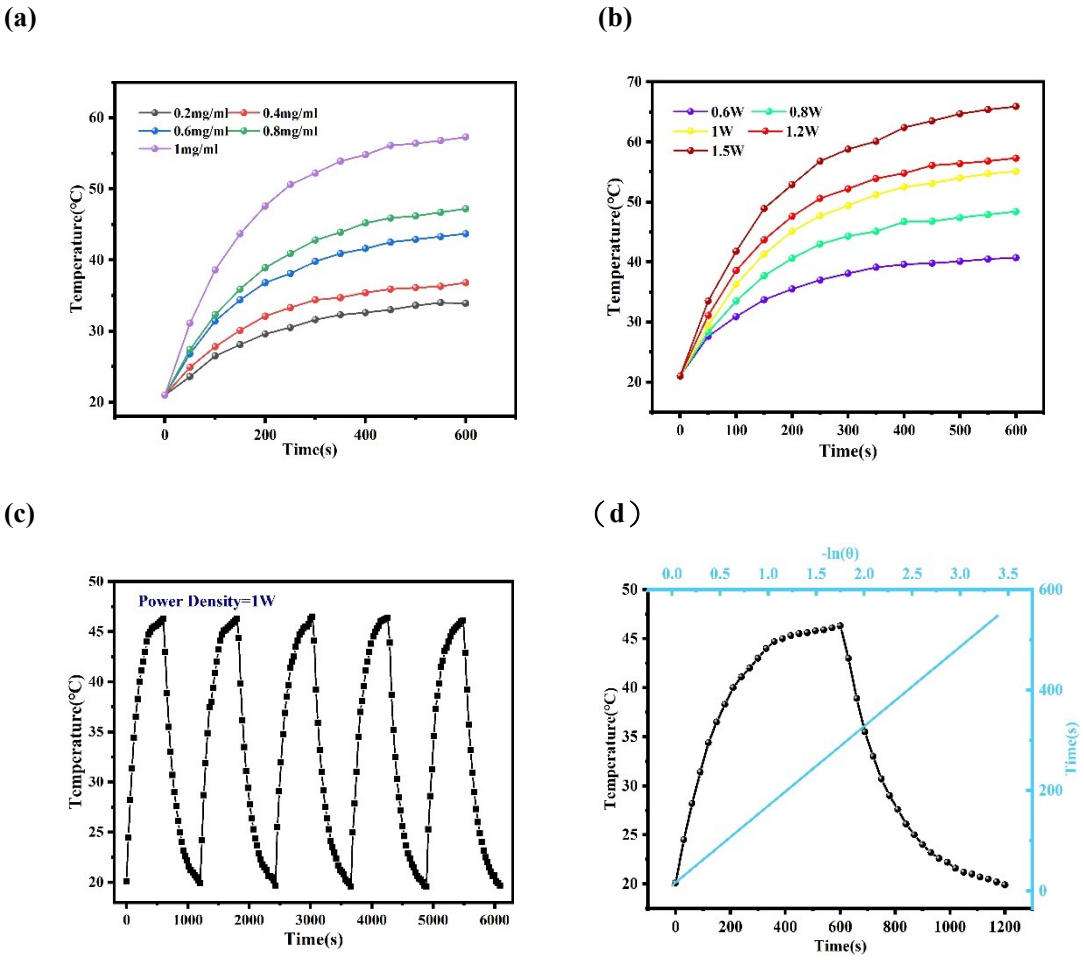

Figure S13 a) Heating curves of the TFCN solution during five laser on/off cycles (808 nm, 1 W cm^{-2}) b) Photothermal conversion efficiency (η) of TFCN solution utilize photothermal heating−cooling cycle. c-d)

The curve of TFCN solution ΔT-NIR irradiation time under different concentration and different light intensities

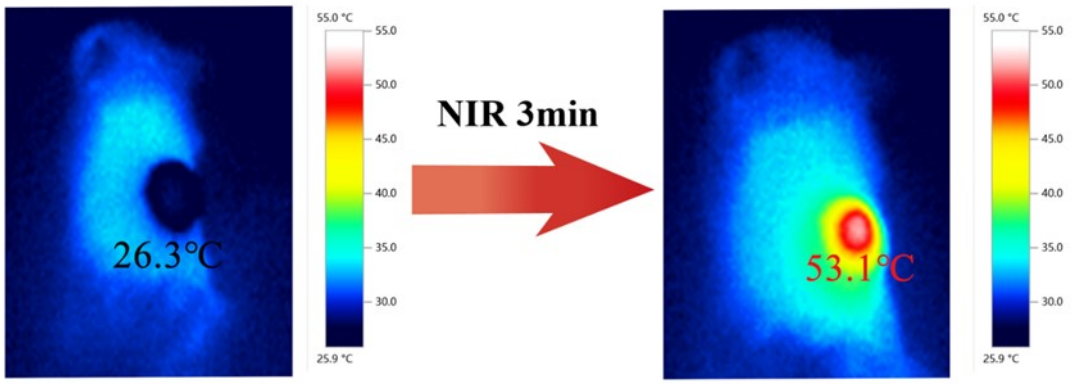

Figure S14 Infrared thermograms of wounds in diabetic mice

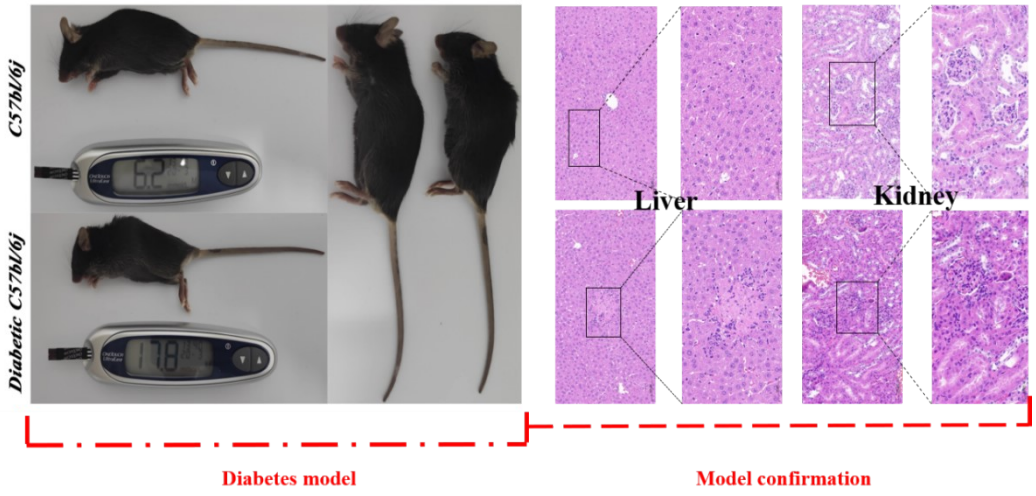

Figure S15The establishment of a diabetic mice model was confirmed by employing hematoxylin and eosin (H&E) staining to assess Liver and Kidney histopathology.

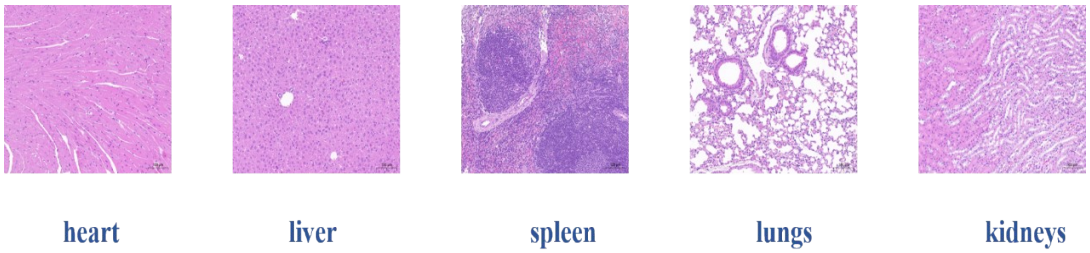

Figure S16 Pathological sections of major organs and biomedical indicators after being treated by hydrogels.(H&E staining images)

Table S1 Formula description of the hydrogel

References:

1. L. Feng, L. Wang, Y. Ma, W. Duan, S. Martin-Saldaña, Y. Zhu, X. Zhang, B. Zhu, C. Li, S. Hu, M. Bao, T. Wang, Y. Zhu, F. Yang and Y. Bu, *Bioact. Mater.*, 2023, **27**, 82-97.
2. H. Dong, L. Wang, L. Du, X. Wang, Q. Li, X. Wang, J. Zhang, J. Nie and G. Ma, *Small*, 2022, **18**, e2201620.
3. M. Fu, Y. Zhao, Y. Wang, Y. Li, M. Wu, Q. Liu, Z. Hou, Z. Lu, K. Wu and J. Guo, *Small*, 2023, **19**, e2205489.
4. M. He, Q. Wang, R. Wang, Y. Xie, W. Zhao and C. Zhao, *ACS Appl. Mater. Interfaces*, 2017, **9**, 15962-15974.
5. D. Xi, M. Xiao, J. Cao, L. Zhao, N. Xu, S. Long, J. Fan, K. Shao, W. Sun, X. Yan and X. Peng, *Adv. Mater.*, 2020, **32**, e1907855.

Components	Alg-PBA(mg)	PVA(mg)	TFCN(mg)	H_2O(mg)
Alg-PBA/PVA	16	32	0	272
$TFCN_{1.1}$-Alg-PBA/PVA	16	32	1.1	272
$TFCN_{1.5}$-Alg-PBA/PVA	16	32	1.5	272
$TFCN_{2.2}$-Alg-PBA/PVA	16	32	2.2	272
$TFCN_{3.0}$-Alg-PBA/PVA	16	32	3.0	272
$TFCN_{4.5}$-Alg-PBA/PVA	16	32	4.5	272